J Wood Sci (1999) 45:254–257

NOTE

Masatoshi Sugimori · Frank Lam

Macro-void distribution analysis in strand-based wood composites using an X-ray computer tomography technique*

Received: August 12, 1998 / Accepted: November 20, 1998

Abstract A database from a series of cross-sectional density distributions in a 0.16 × 0.34 × 1.28 m strand-based wood composite specimen has been successfully developed using X-ray computer tomography (CT) techniques. Using conventional image processing techniques, the CT images of the specimen were analyzed with respect to the size and position of the macro-voids. Finally, CT images and the measurement results were converted and exported into MS Excel spreadsheets to provide information on the three-dimensional distribution of macro-voids so those who are not familiar with image processing and formats can handle the data easily. In future, this type of database can be used to develop a model for the prediction of macro-void presence and distributions in strand-based wood composites.

Key words X-ray · Computer tomography · Strand-based wood composites · Macro-voids

Introduction

Wood-based composite products are engineered material. Their performance is governed by the properties of the wood species, adhesive, manufacturing strategy, and production process. They are formed by arranging flakes, strands, or sheets of veneer and bonding them together with adhesives under heat and pressure to make panels or dimension lumber-like products. The reconstitution process disperses natural defects in the wood, resulting in more consistent and uniform mechanical and physical properties compared to those of solid sawn lumber and more efficient utilization of the fiber resource.

As engineered material, opportunities exist for refinement and optimization of the physical and mechanical properties of wood-based composites through controlling the production parameters. In strand-based wood composites, the presence and distribution of macro-voids are generally governed by the random lengths of the wood strands and their partial random deposition during the forming process. Although the presence and distribution of macro-voids influence the structural and physical properties of strand-based wood composites, their measurement and quantification are difficult; hence, few references are available on the subject. Ellis et al.[1] investigated the measurement of macro-void areas using two imaging systems: a video camera and a line scan camera. Such methods are useful, but they are time-consuming; and the internal presence and distribution of macro-voids cannot be obtained without cutting open the specimens. In this experiment the total nondestructive scanning time, including setting the specimen, was within 60 min.

X-ray computer tomography (CT) can provide the density distribution and the internal structure of the object of interest. Previous work [2–6] has shown that X-ray CT and nuclear magnetic resonance are possible nondestructive scanning techniques to detect defects in log and wood products. The objective of this study is to investigate the use of medical X-ray CT scanning techniques to measure nondestructively the presence and distribution of macro-voids in a strand-based wood composite specimen.

Scanning the 0.18 × 0.35 × 1.82 m strand-based wood composite by CT provided a database from a series of images on the cross-sectional density distribution along the length of the specimen. Image-processing techniques were used to analyze the CT images to obtain the size and location of the macro-voids. The image data were input into an MS Excel spreadsheet format to provide three-dimensional distribution of macro-voids in the specimen so those who are not familiar with image processing and formats could treat the data easily.

M. Sugimori (✉)
Faculty of Agriculture, Ehime University, 3-5-7 Tarumi, Matsuyama 790-8566, Japan
Tel. +81-89-946-3591; Fax +81-89-977-4364
e-mail: sugimori@agr.ehime-u.ac.jp

F. Lam
Department of Wood Science, University of British Columbia, No. 389-2357 Main Mall, Vancouver, BC, Canada V6T 1Z4

*Part of this report was presented at the annual meeting of the Forest Products Society, Vancouver, BC, Canada, June 1997

Materials and methods

CT image and CT number

X-ray CT provides two-dimensional density mapping of cross sections through a material. This image pixel value in CT scans, called CT number, represents the Hounsfield unit, which is related to density as follows:

$$\text{CT number} = 1000 \times (\mu - \mu_w)/\mu_w \quad (1)$$

where μ is the linear attenuation coefficient of the object, and μ_w is the linear attenuation coefficient of water. Air and water correspond to CT numbers of −1000 and 0, respectively. Most wood varies in its CT number from −700 to 0.

Lindgen[7] developed relations between CT numbers and wood density, but these relations cannot be directly applied to other experiments because CT numbers differ among scanners from different manufacturers and even among scanners from the same manufacturer.[8] Therefore, a calibration process is needed where a reference test piece must be scanned using the CT scanner of interest. With knowledge of the volume, moisture content, and oven-dried density of the reference test piece, the relation between the scanner-dependent CT number and density can be obtained precisely.[7] Alternately, in this experiment the average CT number of all the image slices was computed and the dimension and weight of the specimen were measured so the density could be roughly estimated by comparing the measured density with the CT number.

CT scanning and image processing

A series of 128 cross-sectional scans of a commercial strand-based composite member Parallam were obtained with a helical X-ray CT scanner (Xpress/SX, Toshiba Corporation, Tokyo, Japan) at a Vancouver hospital. The CT scanner was set at 120 kV, 200 mA, 10 mm slice thickness, and 0.86 mm pixel size in a 512 × 512 pixel matrix. Routine reconstruction at 512 × 512 was performed at a rate of one image every 3 s. These images included the cross sections of the Parallam specimen and the background. The specimen cross sections were isolated from the background image and their edges trimmed resulting in images of 185 × 400 pixel matrix (0.16 × 0.34 m). They were stored as unsigned 12-bit integers. Accordingly, their values are represented as follows:

$$\text{Image pixel value} = \text{CT number} + 1024 \quad (2)$$

These images were converted to black and white images using a conventional image-processing technique. Dark areas corresponded to macro-voids and light areas to wood substance.

The size and position of macro-voids in each image were then measured with the image-processing software "Image," a public domain software developed by the U.S. National Institutes of Health. It is capable of carrying out most image-processing analyses. The percentage of Parallam area occupied by macro-voids for each CT scan slice was then calculated. After these measurements, the CT images and results were converted and exported to MS Excel spreadsheet format to provide information on the three-dimensional distribution of macro-voids in strand-based wood composites for further research.

Results and discussion

The measured density of the Parallam specimen and average CT number of all CT images are presented in Table 1. Also shown in Table 1 are the maximum, minimum, and standard deviation of the CT numbers. According to this table, adjusting the X-ray CT scanner was not appropriate to obtain the absolute value for density in this experiment, but it was optimized for medical diagnosis. From the defini-

Table 1. Measured density and average, minimum, maximum, and standard deviation of the CT number

Measured density	0.63 g/cm^3
CT number	
Average	−401
Minimum	−1024
Maximum	180
Standard deviation	140

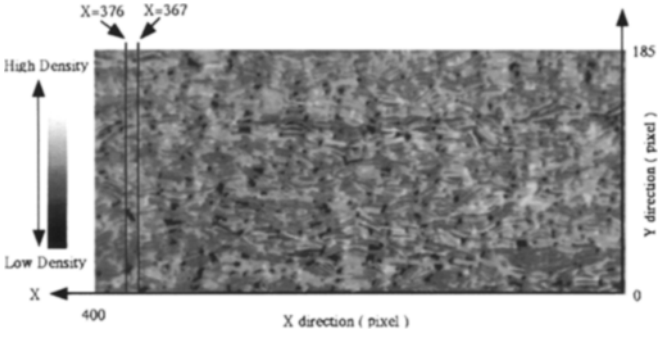

Fig. 1. CT scan of a cross section of a Parallam specimen in which the black areas correspond to macro-voids

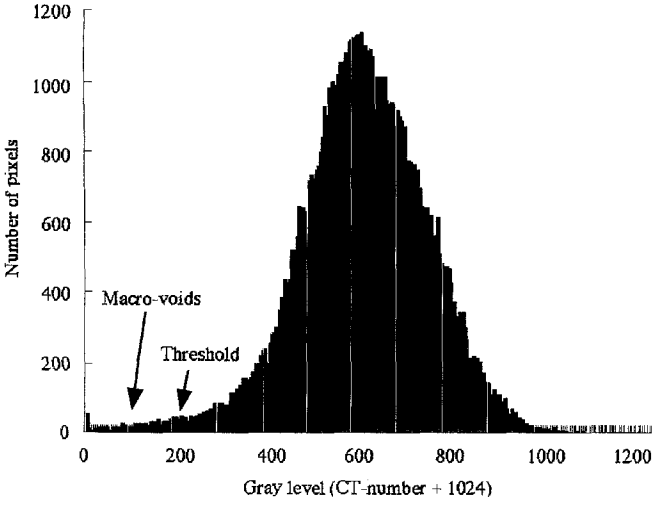

Fig. 2. Histogram showing frequency of pixels for each gray level of the Parallam CT image

tion of macro-voids, defined as spaces among elements in wood composites,[1,9,10] it was assumed that those images had enough contrast to detect macro-voids because each element could be seen on a personal computer display.

An example of a CT slice image is shown in Fig. 1. First, a threshold value had to be determined using a histogram of the gray level. The histogram showing the frequency of pixels for each gray level is shown in Fig. 2. It is difficult to determine the density boundary between wood and macro-voids from this figure; therefore, to study the density boundary, gray level profiles of the area indicated in Fig. 1 (from $X = 367$ to $X = 376$) are compared in Fig. 3. As this area has two macro-voids, it is found that the density boundary lies under 400. We did not determine the density boundary because the precise density of wood substance in this specimen was not known and one pixel of a CT slice image represents the mean density of the box ($0.86 \times 0.86 \times 10$mm). We studied the change of macro-void areas of each slice on a personal computer display while the threshold was changing. Then all the images were converted to binary images using the threshold value of 207. The image in Fig. 1 was converted to the black and white image, as shown in Fig. 4, where black areas correspond to macro-voids and white areas to wood substance.

The number, area, position, major diameter, and minor diameter of the macro-voids (black areas) were then measured by the image-processing software "Image." Figure 5 shows the variation along the length of the Parallam specimen occupied by all macro-voids and macro-voids within 2 pixels. From slice 0 to slice 80, all of the macro-void areas

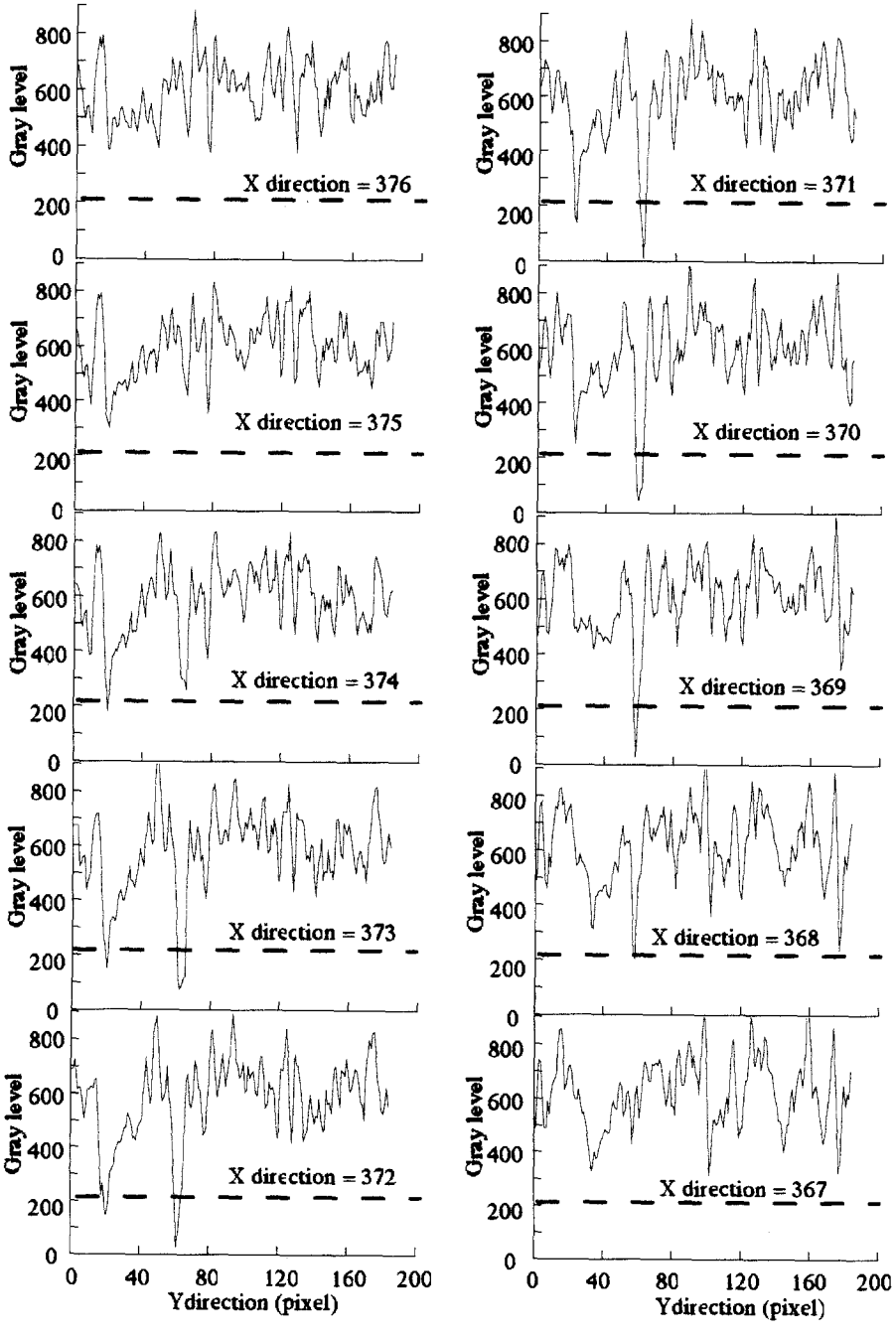

Fig. 3. Gray level profiles of the area indicated in Fig. 1. *X-direction*, from 367 to 376; *dashed lines*, threshold value of 207

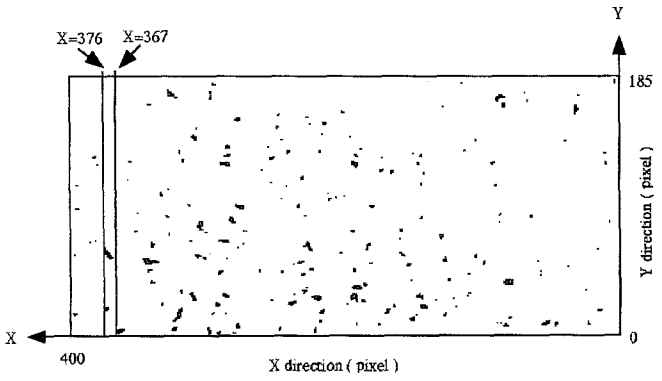

Fig. 4. Black and white image after converting the image in Fig. 1 by a threshold value of 207

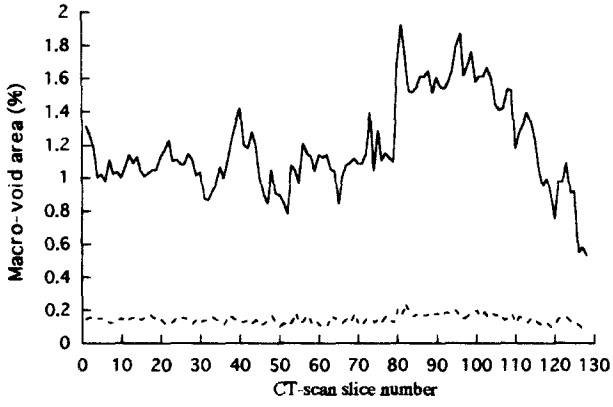

Fig. 5. Variation along the length of Parallam area occupied by macro-voids. *Solid line*, all macro-voids; *broken line*, macro-voids ≤2 pixels

varied in percentage from 0.8% to 1.4%. At slice 80, the percentage of all the macro-void areas increased rapidly to nearly 2% and then gradually fell. The broken line, the same variation occupied by macro-voids within 2 pixels, shows a moderate curve, which implies that the drastic change in the maco-void area is due to the existence of large macro-voids.

Figure 6 is a histogram depicting the distribution of macro-void size. This result agrees with the work of Dai and Steiner,[11] who compared the distribution of void size in a flake layer experimentally measured, computer-simulated, and mathematically predicted.

Conclusions

A database on a series of cross-sectional density distributions in a strand-based wood composite specimen was successfully developed using X-ray CT techniques. Conventional image-processing techniques were used to analyze the CT images of a Parallam specimen with respect to the size and position of its macro-voids. Finally, CT images and

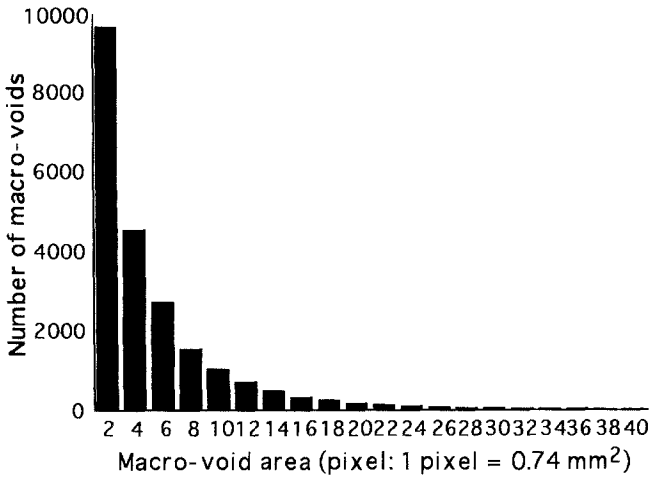

Fig. 6. Histogram depicting the distribution of macro-void size

measurements were converted and exported into MS Excel spreadsheets to provide information on the three-dimensional distribution of macro-voids so those who are not familiar with image processing and formats could treat the data easily. This type of database can be used to develop a model for predicting macro-void presence and distributions in strand-based wood composites.

References

1. Ellis S, Dubois J, Avramidis S (1994) Determination of parallam macroporosity by two optical techniques. Wood Fiber Sci 26(1):70–77
2. Chang SJ, Olson JR, Wang PC (1989) NMR imaging of internal features in wood. For Prod J 39(6):43–49
3. Funt VB, Bryant EC (1985) A computer vision system that analyses CT-scans of sawlogs. In: Proceedings of IEEE computer society conference on computer vision and pattern recognition, San Francisco, June 9–13
4. Funt VB, Bryant EC (1987) Detection of internal log defects by automatic interpretation of computer tomography images. For Prod J 37(1):56–62
5. Taylor FW, Wagner FG, McMillin CW, Morgan IL, Hopkins FF (1984) Locating knots by industrial tomography: a feasibility study. For Prod J 34(5):42–46
6. Wagner FG, Taylor FW, Ladd DS, McMillin CW, Roder FL (1989) Ultrafast CT scanning of an oak log for internal defects. For Prod J 39(11/12):62–64
7. Lindgen LO (1991) Medical CAT-scanning: X-ray absorption coefficients, CT-numbers and their relation to wood density. Wood Sci Technol 25:341–349
8. Levi C, Cray JE, McCullough EC, Hattery RR (1982) The unreliability of CT-numbers as absolute values. Am J Radiol 139:443–447
9. Suematsu A, Okuma M (1988) Mechanism of low-density particleboard formation. I. Hot-pressing process and mechanism of board formation. Mokuzai Gakkaishi 34:820–827
10. Nishimura T, Okuma M (1997) Development of low-density wood based boards considering the distribution of elements. II. Bonding forces and void distributions among elements of wave-element boards. Mokuzai Gakkaishi 43:762–769
11. Dai C, Steiner PR (1994) Spatial structure of wood composite in relation to processing and performance characteristics. Part 2. Modeling and simulation of a randomly-formed flake layer network. Wood Sci Technol 28:135–146